CIRRELT

CIRRELT-2023-15

A Variable Reference Point Many-Objective Approach to Direct Angle and Aperture Optimization in Radiation Therapy Treatment Planning

Ali Fallahi
Mehdi Mahnam
Seyed Taghi Akhavan Niaki
Michel Gendreau

April 2023

Bureau de Montréal
Université de Montréal
C.P. 6128, succ. Centre-Ville
Montréal (Québec) H3C 3J7
Tél : 1-514-343-7575
Télécopie : 1-514-343-7121

Bureau de Québec
Université Laval,
2325, rue de la Terrasse
Pavillon Palasis-Prince, local 2415
Québec (Québec) G1V 0A6
Tél : 1-418-656-2073
Télécopie : 1-418-656-2624

A Variable Reference Point Many-Objective Approach to Direct Angle and Aperture Optimization in Radiation Therapy Treatment Planning

Ali Fallahi[1], Mehdi Mahnam [2,3*], Seyed Taghi Akhavan Niaki [1], Michel Gendreau [3,4]

[1] *Department of Industrial Engineering, Sharif University of Technology, Tehran, Iran*
[2] *Department of Industrial and Systems Engineering, Isfahan University of Technology, Isfahan, Iran*
[3] *Interuniversity Research Centre on Enterprise Networks, Logistics and Transportation (CIRRELT), Montreal, Canada*
[4] *Department of Mathematics and Industrial Engineering, Polytechnique Montreal, Canada*

Abstract. Intensity modulated radiation therapy is one of the widely used methods for cancer treatment worldwide. The beam angle selection, fluence map optimization, and leaf sequencing are the three decision-making problems in IMRT. In this work, we investigate the direct angle and aperture optimization, which addresses the mentioned problems in an integrated framework. According to the conflict in the acceptable level for dose receiving between the tumor and the healthy organs, this problem is inherently multiobjective. We use a multiobjective mixed-integer nonlinear programming model for the problem where the penalty of under and over dose from the prescribed dose for each patient organ is considered as an objective function. Due to the number of objectives and dimensions of the problem, first, we develop three classic many-objective metaheuristic algorithms, NSGA-III, MaOPSO, and NSDE-R, as the solution approaches. To find more acceptable solutions, we develop a new version of many-objective metaheuristic algorithms, which adjust the reference points based on the decision-maker's preferences and the obtained results during the procedure, so-called variable reference point many-objective metaheuristic algorithms. The new approach is implemented for the IMRT treatment problem by integrating a set of non-linear clinical criteria, called dose-volume criteria, as the decision-maker preferences to find more acceptable clinical solutions. We evaluate the performance of the many-objective algorithms using 10 liver cases from the TROTS data set. The results are compared using several computational and clinical criteria. Based on the results, the improved algorithms can successfully consider the preferences without imposing a high computational cost.

Keywords: Intensity modulated radiation therapy, many-objective optimization, dose-volume criteria

* Corresponding author: m.mahnam@iut.ac.ir

1. Introduction

Cancer, as one of the diseases with a high mortality rate, is the result of the abnormal growth of body cells. Several techniques have been used for the treatment of this disease, including surgery, chemotherapy, and radiation therapy. Among these techniques, radiation therapy is one of the widely used methods that at least 50% of cancer patients may experience during their treatment process (Atun et al., 2015). In external radiation therapy, as the most common method, the radiation source is placed outside the cancer patient's body, such as intensity modulated radiation therapy (IMRT) (Ehrgott et al., 2010), and volumetric modulated arc therapy (VMAT) (Dursun et al., 2019). This research focuses on IMRT as one of the most widely used external radiation therapy methods. In IMRT, a linear accelerator (linac) positioned on a gantry delivers radiation to the patient body from various angles. Each beam's intensity is modified using a device on the head of the gantry known as a Multi-Leaf Collimator (MLC). The MLC is composed of two opposing banks of leading and trailing metal leaves that may be automatically moved in the direction of one another. Each beam is also divided into a grid of rectangular shapes called beamlets. A beamlet is thus identified to be open if neither the leading nor the trailing leaves are blocking it, and the intensity is determined by the direction in which the leaves are moving. An efficient treatment plan should be provided to deliver the desired radiation dose to the tumor while simultaneously minimizing the side effects on the healthy organs.

The design of a treatment plan in IMRT requires decision-making in three sub-problems: (1) beam angle optimization (BAO), (2) fluence map optimization (FMO), and (3) leaf sequencing (LS) (Ehrgott et al., 2010). In BAO, a limited number of directions are selected from a set of available beam directions, and the best possible locations are specified for the positioning of the gantry (Ehrgott et al., 2010). The dose intensity map for each selected beam direction is determined by solving the FMO problem (Shepard et al., 1999). In the last phase, a sequencing problem is investigated to determine the leaves' position for delivering the fluence map in a limited set of apertures (Taşkın and Cevik, 2013). These problems were solved sequentially in the classic approach to providing an applicable treatment plan. In this sequential approach, each subproblem's solution quality highly depends on the output quality of the previous subproblem, and the procedure may be very time-consuming for the treatment planner (Hou et al., 2003). Considering these difficulties, researchers tried to address the subproblems in the integrated frameworks. In this way, the beam orientation optimization (BOO) problem was presented by Hou et al. (2003) to integrate the BAO and FMO problems. In addition, the direct aperture optimization (DAO) problem was developed to determine the aperture shapes and intensities, considering a set of given beam directions (Romeijn et al., 2005). Finally, Fallahi et al. (2022b) presented direct angle and aperture optimization (DAAO), in which the selection of beam directions, calculation of intensity map, and the sequencing of MLC are performed simultaneously. They formulated DAAO as a single-objective problem using the quadratic dose penalty objective function, which minimizes the penalty of under and over dose from the prescribed dose for each organ of the patient.

Regarding the dose-receiving conflict between the tumor and healthy organs, the IMRT treatment planning problems fall into the multiobjective optimization problems category. Although the weighted sum method is one of the widely used approaches in the literature, the formulation of problems by using single objective functions significantly reduces the quality of the calculated treatment plan, and increases the computational cost. In this research, we present a multiobjective DAAO problem, in which each patient organ can be considered an objective function based on the oncologist's opinion. The approach provide a set of Pareto treatment plans for the clinical decision-maker. Given the possibility of more than three objective functions, first, we employ the many-objective metaheuristics, the new generation of multiobjective metaheuristics, as the solution approach. Moreover, we develop new variants of many-objective metaheuristics by integrating the preference of decision-makers into the search process. These new versions will be introduced as variable reference point (VR) many-objective metaheuristics. We implement this approach for the multiobjective DAAO problem based on nonlinear Dose Volume Histogram (DVH) criteria, which are common measures used by oncologists to assess the effectiveness of plans in the real world. This approach enables the clinical decision-makers to choose their preferred treatment plan from a Paret set of DVH acceptable plans. In summary, the main contributions of this paper can be expressed as follows:

1. Presenting a multiobjective DAAO problem, in which dose variation penalty for each patient's organs can be considered as an objective function.
2. Designing three classical NSGA-III, MaOPSO, and NSDE-R many-objective metaheuristic algorithms as the solution approach.
3. Developing variable reference point many-objective algorithms, as preference-based many-objective metaheuristics, by integrating decision makers' preferences into the classical algorithms.
4. Utilizing DVH criteria, as clinical decision makers' preferences, to apply variable reference point position metaheuristics to the multiobjective DAAO problem.
5. Evaluating and analyzing the performance of the developed many-objective framework on 10 real liver cases from the TROTS dataset.

The remainder of this paper is organized as follows: In Section 2, the literature on the multiobjective IMRT treatment planning problems is reviewed. In Section 3, the multiobjective DAAO problem is presented and mathematically formulated. In Section 4, three many-objective metaheuristic algorithms are presented as the solution approach, and a new design of these algorithms is developed by integrating the DVH clinical criteria. In Section 5, the efficiency of the algorithms is investigated by solving the problem for 10 real cases of liver cancer, and the computational results are broadly discussed. In Section 6, the research is concluded, and some insights for future studies are proposed.

2. Literature review

The first application of mathematical optimization for radiation therapy treatment planning was proposed by Bahr et al. (1968) using a linear programming model. After, a broad range of operations research applications appeared in radiation therapy treatment planning literature (Mahnam et al., 2019; Lim et al., 2020; Chan and Mišić, 2013; Zaghian et al., 2018). The problem is inherently multiobjective regarding the conflict between the dose received by the tumor and healthy organs and the related criteria. In several works, these objectives are integrated or weighted based on experts' opinions, which finally results in a single objective function. In addition, there are other approaches in the literature which result in a set of non-dominated plans, e.g. Pareto optimality approach. We provide a brief review of these studies, specifically based on heuristic and metaheuristic algorithms, on the IMRT treatment planning literature. More details on optimization methods and multiobjective approaches in radiation therapy treatment planning are available in the comprehensive review papers by Ehrgott et al. (2010),Craft (2013), and Breedveld et al. (2019).

Various metaheuristic algorithms have been proposed for the FMO problem, e.g., simulated annealing (Webb, 1994; Bertsimas et al., 2013), bat algorithm (Kalantzis and Lei, 2014), quantum annealing (Nazareth and Spaans, 2015), and levy-firefly (Kalantzis et al., 2016). Also, there has been an increasing attention to the single-objective integrated problems, including BOO and DAO. For the BOO problem, several heuristic and metaheuristic algorithms, such as conjugate gradient (Li et al., 2005c), ant colony optimization (Li et al., 2005a), particle swarm optimization (Li et al., 2005b), and variable neighborhood search (Freitas et al., 2020), have been proposed. For the DAO problem, several heuristic and metaheuristic single-objective algorithms have been developed, such as genetic (Li et al., 2003), tabu search (Rocha et al., 2012), stochastic local search (Cáceres et al., 2021), differential evolution (Fallahi et al., 2022a), and column generation (Mueller et al., 2022). Recently, Ripsman et al. (2022) has developed a stochastic DAO problem under breathing motion uncertainty. A robust optimization approach was suggested and solved the model via a candidate plan generation heuristic algorithm. Habib et al. (2022) studied a sliding windows IMRT treatment planning, in which the possibility of leaves moving during the dose irradiation time was considered by some deliverability constraints. The presented linear programming model was solved by the CPLEX solver. Moreover, in one of recent works, Fallahi et al. (2022b) developed the single-objective direct angle and aperture optimization (DAAO) as a new integrated model addressing BAO, FMO, and DAO simultaneously. They implemented an adaptive hybrid metaheuristic algorithm as the solution approach for this problem.

The single-objective approach does not necessarily result in clinically acceptable plans and requires trial-and-error with different parameters, which is time-consuming in practice. In fact, there may be a need for several runs to have an acceptable plan from the oncologist's viewpoint. The multiobjective approaches enable the users to choose the preferred plan from a Pareto set of treatment plans without any significant computational effort.

Küfer et al. (2000) first introduced the multiobjective FMO problem, and solved it using a multicriteria algorithm with a special search strategy that does not require the evaluation and comparison of all Pareto solutions. Craft et al. (2007) proposed a two-stage approach for the multiobjective FMO. In this approach, a near-acceptable single solution was calculated as the base of the Pareto approach in the first iteration. Then, they tried to use dosimetry criteria for providing a set of Pareto plans. Shao and Ehrgott (2008) presented a linear multiobjective model for the FMO problem, and solved this model using a sandwich algorithm. Cabrera et al. (2014) considered the multiobjective FMO as a positively homogeneous multiobjective optimization problem. An algorithm was presented in which one of the objective functions is converted to a constraint, and the number of objective functions is reduced. Wilkens et al. (2007) designed a goal programming-based heuristic algorithm to simultaneously address different objective functions in the FMO problem. Jee et al. (2007) solved the multiobjective FMO problem using a lexicographic ordering approach. In this method, the objective functions were categorized to be solved hierarchically. Also, Breedveld et al. (2009) suggested a two-step epsilon constraints algorithm to solve the multiobjective FMO problem.

Based on the multiobjective algorithms proposed for FMO, the multiobjective BOO problem, i.e., the integration of FMO and BAO, has been studied. Schreibmann et al. (2004) first proposed the multiobjective BOO and selected the beam directions using the non-dominated sorting genetic algorithm-II (NSGA-II) algorithm, and estimated the fluence map based on the Shanno algorithm. Fiege et al. (2011) investigated a new design of multiobjective genetic algorithm, called Ferret, for the multiobjective BOO problem. This algorithm was able to solve the BAO and FMO simultaneously. Breedveld et al. (2012) proposed the iCycle algorithm, which takes into account decision-maker's preferences in multi-criteria optimization of beam angles and intensity profiles. Cabrera-Guerrero et al. (2018) solved the multiobjective BOO by combining an exact and a metaheuristic algorithm. A local search algorithm, as a metaheuristic, was responsible for computing the beam directions, and the fluence maps were obtained using an exact algorithm based on the epsilon constraint method. Cabrera-Guerrero and Lagos (2022) presented three local search algorithms for the multiobjective BOO problem. These algorithms had a more reasonable computational time than some previous well-known algorithms.

There are several works that have addressed the multiobjective DAO problem. Lin et al. (2017) formulated the multiobjective DAO problem using a linear model. This work proposed an integrated normal boundary intersection (RNBI)-column generation approach as the solution methodology. In this methodology, RNBI utilizes the column generation to solve a series of linear programming subproblems, which produce a set of Pareto solutions. Cao et al. (2011) designed an NSGA-II algorithm to tackle the multiobjective DAO, and demonstrated that the proposed method is capable of providing acceptable treatment plans. Salari and Unkelbach (2013) proposed a multiobjective column generation algorithm, in which apertures are added sequentially to improve the quality of the Pareto front.

In this paper, we propose a multiobjective DAAO problem, that involves the optimization of beam directions, intensity maps, and aperture shapes simultaneously, where each patient structure can be considered as an objective function. To this end, we develop an efficient many-objective metaheuristic algorithm to provide a set of non-dominated treatment plans. First, we design and implement three classic many-objective metaheuristics, namely NSGA-III, MaOPSO, and NSDER. Next, we introduce new versions of these algorithms that consider decision-makers' preferences during the search process. Finally, we apply the newly developed algorithms to the DAAO problem using the DVH criteria as the preference of medical decision-makers.

3. Problem statement

In this section, we present the mathematical model for the multiobjective DAAO problem. The formulation is an extension of the model proposed by Fallahi et al. (2022a) for the multiobjective framework.

In IMRT treatment planning, there is a set of candidate beam directions $b \in \{1, \dots, B\}$ for positioning the gantry around the couch. The total number of beam directions should not exceed ϖ as an upper threshold. To deliver dose from a beam direction, a sequential set of apertures is required, each is formed by the multileaf collimator. The MLC is assumed as a rectangle with $i \in \{1, \dots, I\}$ rows and $j \in \{1, \dots, J\}$ columns. Each beam is also divided into a grid of beamlets through the intersection of MLC rows and columns. The position variables l_i^k and r_i^k determine the left and right leaves in row i of aperture k. If any of leading or trailing MLC leaves block the beamlet (i, j) of aperture k, then it is blocked, and $x_{ij}^k = 0$. Otherwise, the beamlet is on, i.e., $x_{ij}^k = 1$. According to each aperture k, we assign a binary variable δ_k, which determines whether aperture $k \in \{1, \dots, K_b\}$ is activated or not.

To formulate the dose distribution in patient's body, each structure $s \in \{1, \dots, S\}$ is divided into a set of small cubic volumes $v \in \{1, \dots, V_s\}$, so-called voxels. The dose-influence matrix $D^b_{(i,j)v}$ in Gy/Mu provides an estimate of the dosage that voxel v will receive from beamlet (i, j) at unit intensity, where Gy is the unit of dose intensity (1J/Kg) and Mu is monitor unit.

In summary, the following notations are used in this formulation:

Sets

- S, the set of patient's structures;

- $N \subseteq S$, a subset of structures as objective functions;
- B, the set of candidate beam directions;
- I, the set of available rows in MLC;
- J, the set of available columns in MLC;
- K_b, the set of allowable apertures in beam direction $b \in B$;
- V_s, the set of voxels in structure $s \in S$;

Parameters

- $D^b_{(i,j)v}$, the absorbed dose to voxel v from 1 Gy dose delivered by beamlet (i, j) in direction $b \in B$;
- $\underline{\eta}$, the lower limit on the number of chosen beam directions;
- $\bar{\eta}$, the upper limit on the number of chosen beam directions;
- ϖ, the upper limit for the number of apertures per chosen beam direction;
- R, the upper limit for the dose intensity per aperture;
- $\underline{d}_s$, the underdose threshold for all voxels in structure $s \in S$;
- $\bar{d}_s$, the overdose threshold for all voxels in structure $s \in S$;
- M, a big number;

Variables

- $\theta_b \in \{0, 1\}$, a binary decision variable, with $\theta_b = 1$ if the beam direction b is selected, and $\theta_b = 0$ otherwise;
- y^k, a continuous decision variable, indicating the dose intensity for aperture k;
- $\delta_k \in \{0, 1\}$, a binary decision variable, with $\delta_k = 1$ if the aperture k is selected, and $\delta_k = 0$ otherwise;
- l^k_i, an integer decision variable, showing the left leaf position in row i for aperture k;
- r^k_i, an integer decision variable, showing the right leaf position in row i for aperture k;
- $x^k_{ij} \in \{0, 1\}$, a binary decision variable, with $x^k_{ij} = 1$ if the beamlet (i, j) of aperture k is open, and $x^k_{ij} = 0$ otherwise;
- z_v, a continuous decision variable, showing the received dose of voxel v;

The multiobjective mathematical formulation of the DAAO problem is as follows:

$$Min(f_1(z), \ldots, f_N(z)) \tag{1}$$

Subject to:

$$z_v = \sum_{b\in\mathcal{B}} \sum_{b\in\mathcal{K}_b} \sum_{i=1}^{n_r} \sum_{j=1}^{n_c} D^b_{(i,j)v} x^k_{ij} y_k \qquad \forall v \in \mathcal{V}_s, \forall s \in \mathcal{S} \tag{2}$$

$$\underline{\eta} \leq \sum_{b\in\mathcal{B}} \theta_b \leq \overline{\eta} \tag{3}$$

$$y^k \leq \theta_b \, R \qquad \forall k \in \mathcal{K}_b, \forall b \in B \tag{4}$$

$$\sum_{k\in K_b} \delta_k \leq \varpi \qquad \forall k \in \mathcal{K}_b, \forall b \in B \tag{5}$$

$$l^k_i \leq r^k_i - 1 \qquad \forall k \in \mathcal{K}_b, \forall b \in B, \forall i \in \mathcal{I} \tag{6}$$

$$1 \leq r^k_i \leq J - 1 \qquad \forall k \in \mathcal{K}_b, \forall b \in B, \forall i \in \mathcal{I} \tag{7}$$

$$j x^k_{ij} \leq r^k_i \leq J - 1 \qquad \forall k \in \mathcal{K}_b, \forall b \in B, \forall i \in \mathcal{I}, \forall j \in \mathcal{J} \tag{8}$$

$$(J + 1 - j) x^k_{ij} + l^k_i \leq J \qquad \forall k \in \mathcal{K}_b, \forall b \in B, \forall i \in \mathcal{I}, \forall j \in \mathcal{J} \tag{9}$$

$$\sum_{j=1}^{J} x^k_{ij} = r^k_i - l^k_i - 1 \qquad \forall k \in \mathcal{K}_b, \forall b \in B, \forall i \in \mathcal{I} \tag{10}$$

$$\theta_b \in \{0, 1\} \qquad \forall b \in B \tag{11}$$

$$\delta_k \in \{0, 1\} \qquad \forall k \in \mathcal{K}_b, \forall b \in B \tag{12}$$

$$x^k_{ij} \in \{0, 1\} \qquad \forall k \in \mathcal{K}_b, \forall b \in B, \forall i \in \mathcal{I}, \forall j \in \mathcal{J} \tag{13}$$

$$l^k_i, r^k_i \in Z^{n_r \times K}_+, y \in \mathcal{R}^K_+ \qquad \forall k \in \mathcal{K}_b, \forall b \in B, \forall i \in \mathcal{I} \tag{14}$$

Constraints (2) determine the delivered dose to voxel v of structure s. Constraint (3) restricts the number of selected beam directions to the defined thresholds. Constraints (4) imply that the dose irradiation is only possible for the selected beam directions. These constraints concerning the machine specifications also define the maximum intensity level. Constraints (5) guarantee that there is no dose irradiation from the closed apertures. Constraints (6) specify the limited number of apertures in each beam direction. There is a set of limitations on the sequencing of the leaves. Constraints (7) guarantee that the left leaves in each row be placed before the right leaves, also known as interdigitation constraints. Constraints (8) show the possible position of the right leaves. If a beamlet be blocked by right and left leaves, the related binary of that beamlet should be equal to zero, and this is ensured by constraints (9) and (10), respectively. Conversely, the dose irradiation from the open beamlet is possible, and this is expressed via constraints (11). Finally, the type of the decision variables is presented by constraints (12) to (14).

In this research, we assume that a subset of structures $N \subseteq S$ is taken into account for multiple objectives in the model. To formulate the objective functions, we utilize the least squares objective function, which penalizes the dose received by each voxel of each organ. This objective is commonly used by other researchers and commercial radiation therapy treatment planning systems in practice (Ehrgott et al., 2010; Romeijn et al., 2005; Mahnam et al., 2017). The n^{th} objective function of the problem regarding structure $n \in N \subseteq S$ is formulated as follows:

$$f_n(z) = \sum_{v\in\mathcal{V}_n} [z_v - \underline{d}_s]^2_+ + [\bar{d}_s - z_v]^2_+ \tag{15}$$

where $[\bullet]_+^2$ is the $max\{0, \bullet\}$. In a real MLC device with 16 rows and six columns (Breedveld and Heijmen, 2017), the potential combinations of MLC leaf positions for a single aperture in a beam direction is around 18,477 $\times$ 10^{15}. Although previous research has shown that the objective function is convex (Romeijn et al., 2005), this model is a mixed-integer nonlinear mathematical model based on binary variables in the feasibility space and nonlinearity in the objective function. Due to the model's complexity and size, a multiobjective DAAO approach using commercial solvers or exact algorithms may not produce high-quality treatment plans within a reasonable time and may not be practical (Fallahi et al., 2022b). In the next section, we will discuss the many-objective metaheuristic approaches employed as the solution methodology for the problem.

4. Solution methods

The DAAO problem may involve more than three objectives simultaneously. In such cases, traditional multiobjective metaheuristics may not perform well in searching the solution space. The exponential rise in non-dominated solutions number and the high computational cost of computing performance measures pose challenges to these algorithms in solution spaces with more than three objectives (Deb and Jain, 2013). To address these issues, many-objective metaheuristic algorithms, as a new generation of multiobjective metaheuristics, have been developed and presented in recent years. The many-objective algorithms have been used as the solution approach for a wide range of optimization problems, including knapsack, traveling salesperson, production scheduling, line balancing (Jaszkiewicz, 2018; Fang et al., 2019; Sun et al., 2021; Sahinkoc and Bilge, 2022). Many-objective metaheuristics can be categorized into two approaches: reference point-based algorithms and indicator-based algorithms. Reference point-based algorithms, such as non-dominated sorting genetic algorithm-III (NSGA-III) (Deb and Jain, 2013), many-objective particle swarm optimization (MaOPSO) (Figueiredo et al., 2016), and non-dominated sorting differential evolution algorithm based on reference points (NSDE-R) (Reddy and Dulikravich, 2019), use reference points to balance the trade-off between convergence and diversity and guide the search towards the Pareto front. Indicator-based algorithms, such as indicator-based evolutionary algorithm (IBEA) (Zitzler and Künzli, 2004) and hypervolume-based estimation algorithm (HypE) (Bader and Zitzler, 2010), use indicators such as hypervolume or inverted generational distance for their search process.

In this research, we employ the reference point-based many-objective algorithms as the solution approach for the multiobjective DAAO. To this end, we develop the NSGA-III, MaOPSO, and NSDE-R algorithms, as the many-objectives version of genetic algorithm, particle swarm optimization, and differential evolution. In addition, to improve the algorithm's performance, we propose a new extension of these algorithms by integrating the decision maker's preferences into the search process. To the best of our knowledge, there has been limited attempts to incorporate decision-maker's preferences into the many-objective search procedure. In a related work, Vesikar et al. (2018) proposed a static reference point modification approach to handle preferences in the NSGA-III algorithm. In this approach, the reference point positions are predefined based on the input preferences and are fixed during the algorithm. However, we propose a more general approach that dynamically determines the reference point positions based on search process information and feedback from the algorithm. This approach can handle situations where decision-makers do not have enough information about the desired points. We introduce variable reference point (VR) modified versions of many-objective algorithms as VR NSGA-III, VR MaOPSO, and VR NSDE-R algorithms. Finally, we use the DVH criteria, as the preference of medical decision-makers, to implement the new VR many objective metaheuristics for our multiobjective DAAO problem.

4.1. Reference point-based many-objective algorithms

The use of a set of reference points to direct the algorithm during the search process is the primary characteristic of reference point-based many-objective metaheuristic algorithms. These algorithms employ a systematic simplex lattice design to generate the reference points (Das and Dennis, 1998). These reference points are positioned on a hyperplane that intersects with each objective axis at point 1. Let N denote the number of objectives, and d specifies the division number for each axis. Then, the total number of reference points in set H is calculated as follows:

$$|H| = \binom{N+d-1}{d} \tag{16}$$

In addition to the generation of reference points, two standard steps in the iterations of many-objective algorithms as (1) hyperplane reconstruction using population normalization, and (2) association of the individuals with the reference points. The details of these steps are described in the following sections.

4.1.1. Hyperplane reconstruction using population normalization

Many-objective metaheuristics aim to converge to the Pareto front by repeatedly constructing a hyperplane in each iteration, positioning individuals on it, and associating the positioned individuals with the reference points. Let S_t be the set of available individuals in iteration t. The ideal point z^* includes the best values of all objectives in S_t as $z^* = (z_1^*,z_2^*,\ldots,z_N^*)$. On the contrary, the extreme solution for each objective $i \in N$ is obtained to establish an extreme vector $E = (e_1,e_2,\ldots,e_N)^T$. The solution x_j is called an extreme solution according to i^{th} axis based on the achievement scalarizing function (ASF) as follows:

$$ASF(x_j, w_i) = Max_i(f_i(x_j) - z_i^{min})/w_i \tag{17}$$

where w_i is the weight vector of i^{th} objective. In addition, the intercept vector $(a_1,a_2,\ldots,a_N)$ can be calculated using the following equation:

$$E^{-1}b = \begin{bmatrix} a_1^{-1} \\ a_2^{-1} \\ \vdots \\ a_N^{-1} \end{bmatrix} \tag{18}$$

where $b = (1,1,\ldots,1)^T$. Note that if $rank(E) < N$ or $a_k < 0 \; \forall \; k = 1,\ldots,N$, a_k is set to z_k^{max}, which is the maximum (worst) value of k^{th} objective in the population. Using the ideal point z^* and intercept vector $(a_1,a_2,\ldots,a_N)$, the normalized objective function values of j^{th} individual can be calculated as follows:

$$\hat{f}_i(x_j) = (f_i(x_j) - z_i^*)/(a_i - z_i^*) \tag{19}$$

The pseudo-code for hyperplane reconstruction using population normalization is presented as Algorithm 1.

4.1.2. Association of the individuals with the reference points

After normalizing the population, we assign a reference point to each normalized individual. To this end, we consider a reference line l_h for each reference point $h \in H$, which connects the

Algorithm 1 Hyperplane reconstruction

Require: S_t (Population in iteration t), N (Number of objectives), N_{pop} (Population size)
Ensure: S_t^n (Normalized population in iteration t)

for $i \leftarrow 1$ to N **do**
  Determine the ideal point: $z_i^* = Min_{j \in S_t} f_i(x_j)$;
end for
for $j \leftarrow 1$ to N_{pop} **do**
  for $i \leftarrow 1$ to N **do**
    Translate objective j of individual i: $\hat{f}_i(x_j) = f_i(x_j) - Z_i^*$;
  end for
end for
for $i \leftarrow 1$ to N **do**
  Determine the extreme point for objective i using ASF function in Equation (17);
end for
Determine the intercept vector A using Equation (18);
for $j \leftarrow 1$ to N_{pop} **do**
  for $i \leftarrow 1$ to N **do**
    Normalize objective j of individual i using Equation (19);
  end for
end for

reference point to the origin point. We then compute the perpendicular distance between each individual and its associated reference line as follows:

$$d(x_j, l_h) = ||(x_j - l_h^T x_j l_h / ||l_h^2||)||. \tag{20}$$

Finally, we assign each individual j with the reference point l, with minimum perpendicular distance. Note that multiple individuals may be associated with a reference point, or no individual may be associated with a reference point. The algorithm for this procedure is detailed in Algorithm 2. For instance, the reference points and reference lines on the hyperplane for three objectives are graphically shown in Figure 1.

Many-objective algorithms utilize the normalized individuals and their associated reference points to guide the search process using specific operators based on each algorithm. The details for each algorithm are explained in the following subsections.

Algorithm 2 Association process

Require: S_t^n (Normalized population in iteration t), $|H|$ (Reference points number), N_{pop} (Population size)
Ensure: $\pi(x_j \in S_t^n)$(Nearest reference point), $d(x_j \in S_t^N)$(Distance between individual and nearest reference point)

for $h \leftarrow 1$ to $|H|$ **do**
  Compute the corresponding reference line l_h;
end for
for $j \leftarrow 1$ to N_{pop} **do**
  for $h \leftarrow 1$ to $|H|$ **do**
    Calculate the distance between x_j and l_h;
  end for
  Assign the reference point: $\pi(x_j) = l$: $argmin_{h \in H} d(x_j, l_h)$;
end for

4.1.3. The NSGA-III algorithm

The NSGA-III algorithm, developed by Deb and Jain (2013), is one of the earliest metaheuristics developed specifically for many-objective optimization. The pseudo-code for the NSGA-III algorithm is provided in Algorithm 3.

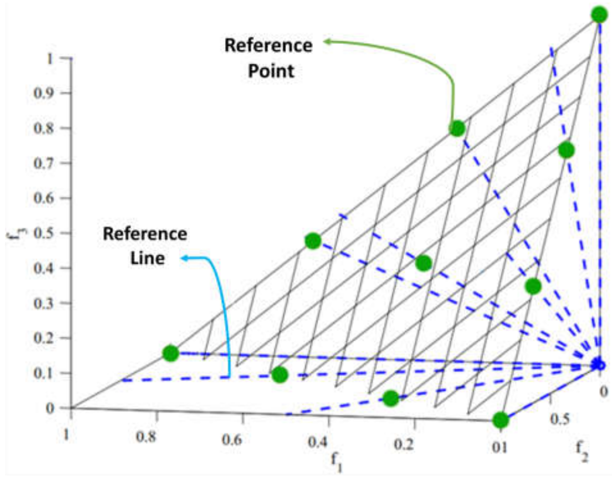

Figure 1: The positioning of reference points and lines on the hyperplane for three objectives

At the t^{th} iteration of NSGA-III, the population S_t generates the offspring population Q_t using the crossover and mutation operators (lines 2-4). These operators use predefined crossover probability P_{cr} and mutation probability P_{mu} parameters, as proposed by Deb et al. (2002). Using the non-dominated sorting operator, the combined population $P_t = S_t \cup Q_t$ is categorized into non-dominated fronts (lines 5-6). The individuals are then gradually added to the next iteration parent population S_{t+1}, based on the order of fronts, until the size of S_{t+1} becomes larger than or equal to population size N_{pop} (lines 7-10).

After adding the individuals from front l to S_{t+1}, if $|S_{t+1}| = N_{pop}$, all selected solutions become the parents' population S_{t+1}, and the algorithm proceeds to the next iteration. However, if $|S_{t+1}| > N_{pop}$ (line 11), all solutions from the previous $l-1$ fronts are selected for inclusion in the next parent population S_{t+1} (line 12). Then, $N_{pop} - |S_{t+1}|$ parents should be selected from the front F_l. The algorithm selects the remaining individuals using a niche preservation operator. To this end, the hyperplane reconstruction and individual association steps are performed (lines 13-14).

NSGA-III defines the niche count parameter ρ_h as the number of associated individuals from S_{t+1}/F_l for each reference point $h \in H$ (line 15) and determines $H_{min} = Min_{h \in H} \rho_h$ as the set of reference points with minimum ρ_h (line 16). A reference point $\bar{j}$ should be randomly selected from H_{min} (line 17). If $\rho_{\bar{j}} = 0$ (line 18), it means no individual in previous fronts are associated with this reference point. There are two possible scenarios with respect to the number of individuals associated with reference point $\bar{j}$ in the current front l: (1) At least one individual in the current front l is associated with $\bar{j}$. In this case, the individual with the minimum perpendicular distance to $\bar{j}$ is selected. Then, the value of $\rho_{\bar{j}}$ is increased by one (lines 19-21). (2) No individual in the current front l is associated with $\bar{j}$. In this case, the reference point $\bar{j}$ is excluded from consideration for individual selection in this iteration (lines 22-23). When $\rho_{\bar{j}} \geq 1$, at least one individual $\bar{j}$ in previous fronts is associated with this reference point (line 25). In this case, one of the individuals in the current front is selected randomly. Note that when an associated individual is selected, the $\rho_{\bar{j}}$ is increased by one (lines 26-27).

4.1.4. The MaOPSO algorithm

The MaOPSO algorithm, introduced by Figueiredo et al. (2016), is the many-objective extension of the PSO algorithm. The pseudo-code of this method is provided in Algorithm 4.

Unlike NSGA-III, MaOPSO uses an external archive, denoted by A_t, in each iteration t to store

Algorithm 3 NSGA-III algorithm

Require: Max_{it} (Maximum iteration), N_{pop} (Population size), P_{cr} (Crossover probability), P_{mu} (Mutation probability), S_0 (Initial population), $|H|$ (Reference points number)
Ensure: $S_{Max_{it}}$ (Final population)

```
1: for it ← 1 to Max_it do
2:     Apply crossover operator using crossover probability P_cr;
3:     Apply mutation operator using mutation probability P_mu;
4:     Generate offspring population Q_t;
5:     Establish combined population P_t = S_t ∪ Q_t;
6:     Sort individuals in non-dominated fronts F_1,F_2,..;
7:     while |S_{t+1}| ≥ N_pop do
8:         S_{t+1} = S_{t+1} ∪ F_l
9:         l = l + 1;
10:    end while
11:    if |S_{t+1}| > N_pop then
12:        S_{t+1} = ∪_{i=1}^{l} F_i;
13:        Reconstruct Hyperplane using population normalization;
14:        Associate individuals with the reference points;
15:        Compute niche count for each reference point h ∈ H;
16:        Determine the set of reference points with minimum niche count H_min = Min_{h∈H} ρ_h;
17:        Select a random reference point in H_min as j̄;
18:        if ρ_j̄ = 0 then
19:            if There is at least one individual in front l that is associated with j̄ then
20:                Select the individual with minimum perpendicular distance distance to j̄;
21:                ρ_j̄ = ρ_j̄ + 1;
22:            else
23:                Exclude j̄ for individual selection in iteration t;
24:            end if
25:        else
26:            Select one of the associated individuals to j̄ randomly;
27:            ρ_j̄ = ρ_j̄ + 1;
28:        end if
29:    end if
30: end for
```

the non-dominated solutions. This archive is updated using the positions of the particles and the latest archive (line 2).

The algorithm updates the hyperplane and associates particles with reference points using the ideal and intercept points obtained from external archive A_t (lines 6-7). Subsequently, MaOPSO computes density measure μ_a and convergence measure ρ_a for each particle $a \in A_t$ to select the global best positions $Gbest_i^t$ and prune the archive. Assuming that individual a associated with the reference point j, the density measure μ_a denotes the total number of associated particles to reference points j (line 9). In addition, the convergence measure of the solution a is the corresponding value of the ASF function, which is calculated using Equation (17) (line 10). To select $Gbest_i^t$, the algorithm divides particles into two sub-populations, S_1^t and S_2^t (line 12). For each particle $i \in S_1^t$, the algorithm assigns the extreme solutions of the archive as $Gbest_i^t$.

Let $\Omega = e_1, e_2, \ldots, e_N$ be the set of N extreme solutions where $\Omega \subset A_t$. These extreme solutions are uniformly assigned to the particles in sub-population S_1^t (lines 13-15). For sub-swarm S_2^t, the algorithm simultaneously uses density and convergence measures to assign $Gbest_i^t$. Assuming i and j are the indices of two solutions randomly selected from the external archive. If $\mu_j < \mu_k$, the algorithm selects solution j as the global best position of the particle. However, if $\mu_j = \mu_k$, the convergence measure is used for comparison. In this case, solution i is selected as the global best

Algorithm 4 MaOPSO algorithm

Require: Max_{it} (Maximum iteration), N_{pop} (particle number), w (Inertial weight), c_1 (Cognitive parameter), c_2 (Social parameter), w_{damp} (Weight modification factor), S_0 (Initial population), A_0 (Initial archive), $|H|$ (Reference points number), $Arch_{size}$ (Archive size)
Ensure: $A_{Max_{it}}$ (Last generation archive)
1: **for** $t \leftarrow 1$ to Max_{it} **do**
2: Update external archive: $A_t = A_{t-1} \cup S_{t-1}$;
3: **if** $|A_t| > Arch_{size}$ **then**
4: Prune archive using density and convergence measures μ_a and ρ_a;
5: **end if**
6: Reconstruct hyperplane using population normalization;
7: Associate the particles with the reference points;
8: **for** $a \leftarrow 1$ to $Arch_{size}$ **do**
9: Calculate the density measure μ_a for particle a;
10: Calculate the convergence measure ρ_a for particle a;
11: **end for**
12: Divide the population into two sub-population S_1^t and S_2^t;
13: **for** $j \leftarrow 1$ to $|S_1^t|$ **do**
14: Select $Gbest_j^t$ from the extreme points;
15: **end for**
16: **for** $j \leftarrow 1$ to $|S_2^t|$ **do**
17: Select $Gbest_j^t$ from the archive using density and convergence measures;
18: **end for**
19: **for** $j \leftarrow 1$ to N_{pop} **do**
20: **if** Current position dominates of particle j the previous position **then**
21: Set the current position as $Pbest_j^t$ for particle j;
22: **else if** Previous position of particle j dominates the current position **then**
23: Set the previous position as $Pbest_j^t$;
24: **else**
25: Set the position minimum perpendicular distance as $Pbest_j^t$;
26: **end if**
27: **end for**
28: **for** $j \leftarrow 1$ to N_{pop} **do**
29: Update the velocity of particle j;
30: Update the position of particle j;
31: **end for**
32: Apply polynomial mutation operator;
33: **end for**

position if $\rho_j < \rho_k$ (lines 16-18).

To determine the personal best position $Pbest_i^t$ of each particle i, the algorithm compares the current and previous positions of particles based on their objective functions. If either of the two positions dominates the other, it is selected as $Pbest_i^t$, (lines 20-23). If two positions are non-dominated with respect to each other, the algorithm chooses the position with the lower perpendicular distance to the ideal point as $Pbest_i^t$ (lines 24-25).

Finally, the MaOPSO algorithm updates the particles' position in the solution space using the assigned global and personal best positions (lines 28-31). To prevent premature convergence and maintain diversity, a polynomial mutation is applied to 15% of the particle population (line 32). If the number of solutions in the archive exceeds its capacity, the archive is truncated at the beginning of the next iteration. (lines 3-5). The algorithm prioritizes the density measure when truncating the archive, and employs the diversity measure if two solutions are incomparable in terms of the density measure.

4.1.5. The NSDE-R algorithm

Reddy and Dulikravich (2019) proposed the NSDE-R algorithm, a many-objective DE algorithm. The pseudo-code for NSDE-R is presented in Algorithm 5.

Algorithm 5 NSDE-R algorithm

Require: Max_{it} (Maximum iteration), N_{pop} (Population size), F (Mutation scale factor), P_{cr} (Crossover probability), S_0 (Initial population), $|H|$ (Reference points number)
Ensure: $S_{Max_{it}}$ (Final population)
1: **for** $it \leftarrow 1$ to Max_{it} **do**
2: Apply classical and convex mutation operators using mutation scale factor F;
3: Apply crossover operator using crossover probability P_{cr};
4: Reconstruct hyperplane using population normalization;
5: Associate the individuals with the reference points;
6: Sort the individuals in non-dominated fronts F_1,F_2,..;
7: **while** $|S_{t+1}| \geq N_{pop}$ **do**
8: $S_{t+1} = S_{t+1} \cup F_l$;
9: $l = l + 1$;
10: **end while**
11: **if** $|S_{t+1}| > N_{pop}$ **then**
12: $S_{t+1} = \cup_{i=1}^{l} F_i$;
13: Compute niche count ρ_h for each reference point $h \in H$;
14: Determine the set of reference points with minimum niche count $H_{min} = Min_{h \in H} \rho_h$;
15: Select a random reference point in H_{min} as $\bar{j}$;
16: **if** $\rho_{\bar{j}} = 0$ **then**
17: **if** There is at least one individual in front l that is associated with $\bar{j}$ **then**
18: Select the individual with minimum perpendicular distance distance to $\bar{j}$;
19: $\rho_{\bar{j}} = \rho_{\bar{j}} + 1$;
20: **else**
21: Exclude $\bar{j}$ for individual selection in iteration t;
22: **end if**
23: **else**
24: Select one of the associated individuals to $\bar{j}$ randomly;
25: $\rho_{\bar{j}} = \rho_{\bar{j}} + 1$;
26: **end if**
27: **end if**
28: **end for**

At the t^{th} iteration of NSDE-R, the parent population S_t generates the offspring population Q_t by applying the classical and convex mutation operators of the DE algorithm (line 2). In addition, a crossover operator is utilized based on a crossover probability P_{cr} (line 3). After, the hyperplane is reconstructed using normalized objective values of the combined population $P_t = S_t \cup Q_t$ (line 4). Each individual in the combined population P_t is associated with a reference point (line 5). The combined population P_t is then sorted into non-dominated fronts (line 6). Based on the order of fronts, the individuals are gradually added to the next iteration population S_{t+1}, until $|S_{t+1}| \geq N_{pop}$ (lines 7-10). If $S_t = |N_{pop}|$, the added solutions are chosen as the next iteration population, and the algorithm proceeds to the next iteration. However, if $S_t > |N_{pop}|$, the solutions from the previous $l - 1$ layers are retained in S_{t+1} (line 12). Similar to the NSGA-III algorithm, $|N_{pop}| - P_{t+1}$ individuals should be chosen from the last layer F_l using a niche preservation operator.

After the association, $\rho_{\bar{j}}$ should be increased by one (lines 23-25).

In the NSDE-R algorithm, the number of associated individuals from $S_{t+1} = S_{t+1}/F_l$ to the reference line h is the niche count ρ_h of the corresponding reference point (line 13). The algorithm identifies the set of reference points with the minimum ρ_h as $H_{min} = Min_{h \in H} \rho_h$ (line 14). Next, the algorithm selects a random reference point in the set H_{min} as $\bar{j}$ (line 15). If $\rho_{\bar{j}} = 0$ and there is at least one associated point in front F_l, the algorithm selects the solution with the shortest perpendicular distance to $\bar{j}$ for adding to S_{t+1}, and $\rho_{\bar{j}}$ is incremented by one (lines 17-19). If there is no associated point in the last front l, the reference point is not considered for selecting individuals (lines 20-21). In the case of $\rho_{\bar{j}} \geq 1$, a randomly selected individual from front l is associated with this reference point and added to P_{t+1}. After the association, $\rho_{\bar{j}}$ should be increased by one (lines 23-25).

4.2. Variable reference point many-objective algorithms

The classic many-objective metaheuristic algorithms employ evenly distributed reference points to compute Pareto solutions with the maximum possible diversity. However, in practice, the decision-makers may prefer particular regions or solution in the Pareto front. In other words, they may be interested in Pareto solutions with certain features rather than an entire Pareto front estimation with a high level of diversity. The IMRT treatment planning problem is a clear example, where the oncologists prefer the clinically acceptable solution to many other impractical solutions in the Pareto front, while these preferences are not considered in the model due to their complexity. In this problem, some non-dominated treatment plans can not be used in practice due to the lack of dose delivered to the tumor. Thus, we propose a variable reference point (VR) extension of the many-objective algorithms to integrate decision-maker's preferences into the traditional many-objective metaheuristics. This framework will be presented in the next section. Then, we provide our approach to implement the VR framework for the multiobjective DAAO problem.

4.2.1. The proposed variable reference point framework

The aim of the proposed VR framework is to modify the classic many-objective approach by dynamically adjusting the position of reference points during the search process based on the decision-maker's criteria for obtaining results.

Consider a set of V desired points in a N objective space problem. The decision maker should determine their desired objective values for each point as an input matrix of size $G_{V\times N}$.If the decision-maker is uncertain about the preferred points at the beginning of the process, these points can be randomly initialized. However, the priority of objective functions for each desired point should be determined as an input matrix $P_{V\times N}$. This matrix includes binary values from 1 to N, where the objective with the highest priority is assigned 1, and N is assigned to the lowest priority objective. Then, the desired point $v \in V$ is normalized using the normalization Equation (19), and the normalized value is denoted by $\hat{v}$. The projection of $\hat{v}$ onto the hyperplane is calculated by determining a reference line, which connects the ideal point to $\hat{v}$ as follows:

$$u_{\hat{v}} = \frac{\sqrt{N}(e_0 - z_0)}{\hat{f}v.(1, ..., 1)^T}.f_{\hat{v}} + z_0, \tag{21}$$

where z_0 is the initial ideal point, e_0 is one of the extreme points such as $(1,0,\ldots,0)^T$. Then, the initial $|H|$ reference points are transformed around the normalized desired point. The algorithm obtains the center of gravity of reference points as follows:

$$c = \frac{\sum_{h=1}^{|H|} h}{|H|}. \tag{22}$$

Then, the transformation of the reference points around $\hat{v}$ is computed with respect to value c as follows:

$$Q_{\hat{v}} = (u_{\hat{v}} - c) + \alpha_{\hat{v}} \times H \tag{23}$$

where $\alpha_{\hat{v}}$ is a shrinkage factor that controls the focus of $|H|$ reference points around the desired points $\hat{v}$. A higher value of $\alpha_{\hat{v}}$ results in a tighter clustering of the reference points around the desired point. This procedure is repeated for all V normalized desired points.

As previously mentioned, the decision-maker may not have sufficient information about the precise objective values of preferred solutions. Additionally, they may specify certain regions that not be accessible for the algorithm. Therefore, the positions of initially generated reference points are assumed to be variable. This ensures that the algorithm explores the desired region and its neighborhood as much as possible. For this goal, the desired points are adjusted at specific stages of the search process.

The many-objective algorithm stores the best solutions for each objective function in an external archive. Then, according to the priority matrix P for each desired point, the algorithm assigns values to the objectives. We refer to the modification of the algorithms based on this procedure as VR NSGA-III, VR MaOPSO, and VR NSDE-R algorithms. The general pseudo-code of the presented scheme is provided in Algorithm 6.

Algorithm 6 The proposed variable reference point many-objective framework

```
Require: V (Set of desired points), α (Set of shrinkage factors), P (Priority matrix), |H| (Reference points number)
for v ← 1 to V do
    Normalize desired point v using Equation (19);
    Project normalized desired point v̂ on the hyperplane using Equation (21);
    Compute the centre of gravity c using Equation (22);
    Transform reference point set H around the desired point projection v̂ using Equation (23);
end for
Execute the many-objective algorithm;
if Position update is necessary then
    for v ← 1 to V do
        Update the desired point v using the priority matrix P;
        Normalized desired point v using Equation (19);
        Project normalized desired point v̂ on the hyperplane using Equation (21);
        Compute the centre of gravity c using Equation (22);
        Transform reference point set H around the desired point v̂ using Equation (23);
    end for
end if
```

A general overview of the proposed procedure is also graphically shown in Figure 2. In this example, there are two desired points with two sets of corresponding reference points. The many-objective algorithm updates the position of two desired points once every ten iterations. Then, the reference points are transformed around the projection of the updated desired points.

4.2.2. Variable reference point framework implementation for multiobjective DAAO

In this section, we present our VR many-objective approach to the multiobjective DAAO problem using DVH criteria, with the aim of improving the algorithm's performance in obtaining clinically acceptable plans. The DVH diagram is one of the most commonly used tools the oncologist utilizes to evaluate the quality of treatment plans. This diagram shows the relationship between the structure's volume and the radiation dose, by determining the percentage of the structure which receives a certain dose or above that. For example, $V_y = x$ states that no more than $x\%$ of the structure receives radiation doses more than y Gy. As explained before, the VR many objective algorithms need a set of desired points as the input to search for the solutions. According to the importance of clinical criteria in the multiobjective DAAO problem, we employ DVH points

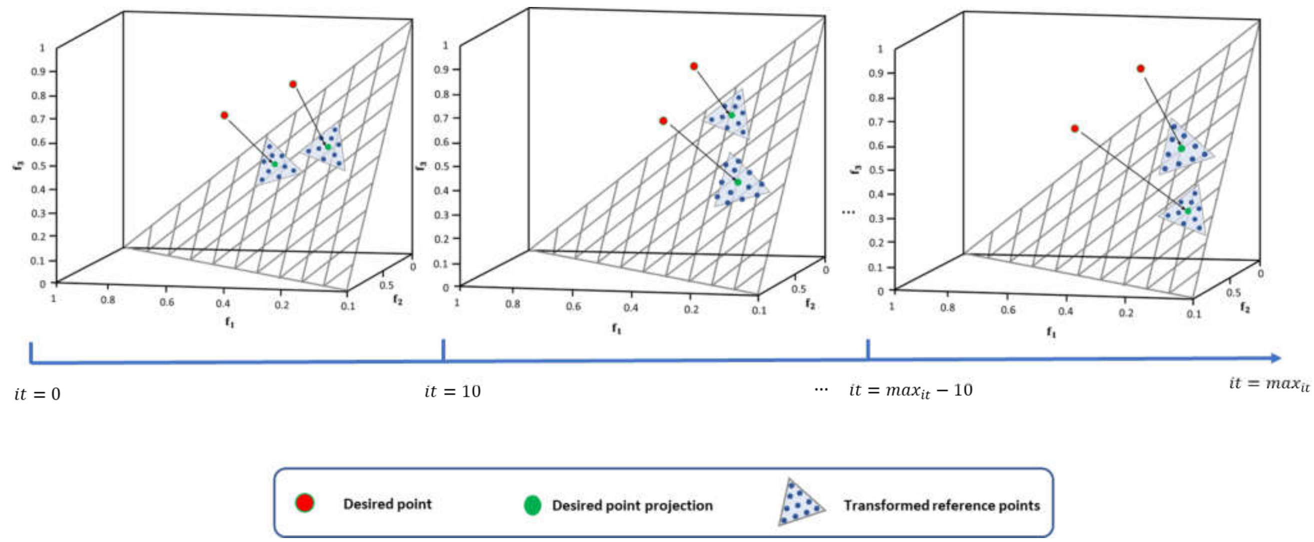

Figure 2: A general overview of the proposed procedure for VR many-objective algorithms

as the input desired points for the algorithms. These points will guide the optimization process towards achieving the desired dose-volume constraints that are critical for patient treatment.

Since the exact corresponding objective values of desired DVH points are unknown, we randomly initialize a set of desired points. To determine the priorities of DVH for each desired point, we use a priority matrix P. For instance, the first desired point can be assigned to the non-dominated solution with the best DVH value for the tumor objective. Similarly, other points can be assigned to the DVH points for the other structures. During the search process, the algorithm updates the objective values of these points and the position of reference points with respect to the priority of DVH points for structures.

4.3. Solution encoding

An appropriate solution encoding scheme is necessary to ensure the efficiency of the metaheuristic algorithm. One challenge in solving the presented DAAO problem is the sequential dependency of problem variables. This work uses a six-vector hierarchical solution encoding for the problem. The vectors represent the number of beam directions, the set of selected beam directions, the number of apertures, the apertures' intensities, and the position of the left and right leaves. Figure 3 shows the solution encoding for an individual in the population. Since the simultaneous assignment of values to the vectors is not possible, the operators are applied based on the order of vectors. First, the number of beam directions is determined. Then, the set of beam angles is specified based on the number of beam directions. This procedure continues until the left and right leaves position for each aperture of each direction is determined.

5. Computational results

This section investigates the performance and efficiency of the presented multiobjective model and many-objective metaheuristic algorithms using a real-world data set of cancer patients. All many-objective metaheuristics are implemented in MATLAB R2017b language and executed on a computer equipped with an Intel Xeon E312 CPU and 64 GB RAM.

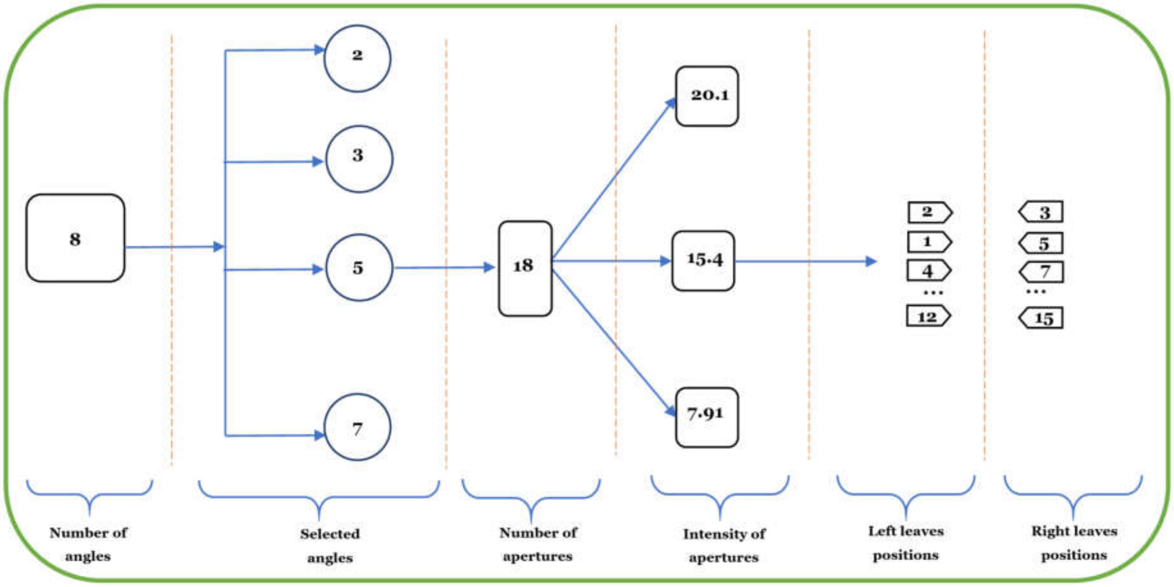

Figure 3: The solution encoding scheme

5.1. *Data description*

We evaluate the performance of the proposed model and algorithms using real-world data from The Radiotherapy Optimisation Test Set (TROTS) dataset (Breedveld and Heijmen, 2017). We use the liver cases from TROTS, which consist of 10 patients. In this study, we consider the spinal cord, heart, and right kidney as the primary healthy organs in the problem. Thus, the least square objective of planning target volume (PTV) and the three healthy organs are the four objective functions of the problem. The acceptable threshold for the PTV of all liver cases is considered to be between 55 and 75 Gy (Breedveld et al., 2019). In addition, maximum 1% of the spinal cord and heart should receive a dose upper than 18 Gy and 30 Gy, respectively. For the right kidney, no more than 35% of the organ can receive a maximum dose of 15 Gy. The dose delivery intensity is constrained to be within the interval of $[0, 25]$ (MUs/aperture). The treatment process is implemented during 14 fractions, where a 5 Gy dose should be delivered to the tumor per each fraction.

5.2. *Performance measures*

For many-objective algorithms, which report a set of non-dominated solutions, objective function values cannot be directly employed to compare the algorithms' performance. Several measures are commonly used for comparing the performance of multiobjective algorithms. A comprehensive discussion of these measures is presented in Audet et al. (2021). In this study, we use the following four measures to evaluate the many-objective algorithms and gain insights into their solutions:

1. Overall non-dominated vector generation measure: This measure indicates the number of solutions in an estimated Pareto front by the algorithm. The higher values for the overall non-dominated vector generation measure are more acceptable.

2. Diversity measure: The diversity measure evaluates the spread of solutions in an estimated

Pareto front. This measure is obtained as follows:

$$Diversity(X) = \sum_{i=1}^{|X_N|} max(|x_i - y_i|) \tag{24}$$

where $|x_i - y_i|$ is the Euclidean distance between two adjacent solutions on the estimated Pareto front. The higher values for the diversity measure are more acceptable.

3. Spacing metric: The Spacing metric quantifies the variability in the distances between solutions in the Pareto front approximation set. Let X be the set of Pareto solutions generated by a multiobjective algorithm. The spacing metric for the solutions in X is as follows:

$$Spacing(X) = \sqrt{(\frac{1}{|X_N| - 1}) \sum_{i=1}^{|X_N|} (\bar{d} - d_1(x_i, X_N \backslash \{x_i\}))^2} \tag{25}$$

where $d_1(x_i, X_N \backslash \{x_i\}) = min_{x \in X_n \backslash \{x_i\}}(||x - x_i||)_1$ is the distance of $x_i \in X_n$ to the $X_N \backslash \{x_i\}$ set. In addition, $\bar{d}$ is the average of all $d_1(x_i, X_N \backslash \{x_i\})$ for $i = 1, .., |X_N|$. The lower values for the spacing measure are more acceptable.

4. CPU time measure: This metric calculates the required time of an algorithm to solve the problem. CPU time measure is used to compare the computational cost of algorithms. The lower values for the CPU time measure are more acceptable.

5.3. Parameter calibration

The value of input parameters highly impacts the efficiency of metaheuristics. In this situation, the trial-and-error-based approaches may be very time-consuming and they do not guarantee a proper performance level of algorithms. We employ the Taguchi design of experiments (DEO), as one of the well-known and simplest statistical approaches, which is successfully used for parameter tuning of a wide range of metaheuristic algorithms in the literature. Taguchi divides the affecting factors on a response variable into two groups signal (S)0 factors and noise (N) factors. Then, a series of experiments are designed to determine the best level of S factors in such a way that the response value is optimized. To control the experiment's number, orthogonal arrays are used by Taguchi instead of a full factorial design. Analysis of variance (ANOVA) and analysis of signal-to-noise ratio (S/N) are two approaches that are used to analyze the results of experiments (Sadeghi et al., 2014). While ANOVA can be only used for experiments with one replication, the S/N analysis approach can be applied for experiments with multiple replications. The results of metaheuristics vary among runs regarding their inherent random behavior. Therefore, we tune the parameters using the S/N ratio, which is calculated as follows for a minimization problem:

$$S/N = -10 \log(\sum_{j=1}^{k} (y_j^2)/k) \tag{26}$$

where y_j is the value of response in j^{th} replication, and k is the total number of replications. The algorithms and the three levels considered for optimization are presented in Table 1.

Table 1: The three considered levels of many-objective algorithms for parameter tuning

Many-objective algorithm	Number	Name	Level 1	Level 2	Level 3
NSGA-III & VR NSGA-III	1	N_{pop}	20	25	30
	2	$\|H\|$	30	45	60
	3	P_{cr}	0.70	0.90	0.95
	4	P_{mu}	0.10	0.50	0.70
MaOPSO & VR MaOPSO	1	N_{pop}	20	25	30
	2	$Arch_{size}$	30	35	40
	3	$\|H\|$	30	45	60
	4	C_1	1	1.5	2
	5	C_2	1.5	2	2.5
	6	w	0.90	0.95	0.99
	7	w_{damp}	0.95	0.99	1
NSDE-R & VR NSDE-R	1	N_{pop}	20	25	30
	2	P_{cr}	0.90	0.95	0.99
	3	$\|H\|$	30	45	60
	4	F	0.50	0.90	1.40

Case #1 from the dataset is used as the input problem for all six algorithms. We run each orthogonal array in five replications. In each replication, the spacing measure is considered as the response variable (Shahidi-Zadeh et al., 2017). To ensure a fair comparison and equal access of algorithms to computational resources, we set the number of function evaluations (NFE) to 1500 as the stopping criterion. The main effects plots of S/N ratio are provided in Figure 4. In these figures, the optimal level is the one with the highest mean of S/N. In addition, the obtained optimal parameter levels are summarized in Table 2.

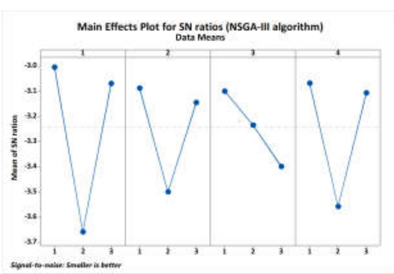

(a) NSGA-III algorithm

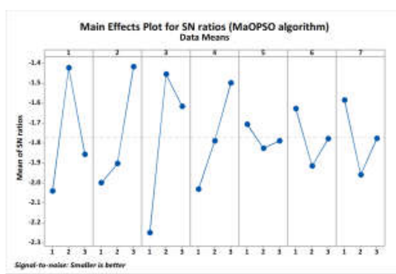

(b) MaOPSO algorithm

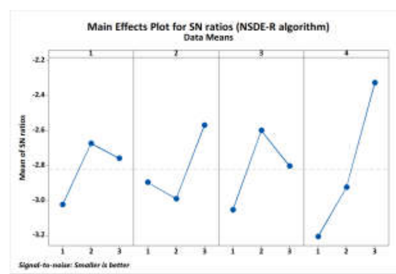

(c) NSDE-R algorithm

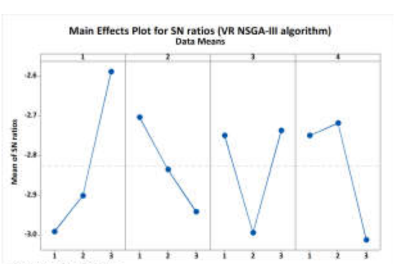

(d) VR NSGA-III algorithm

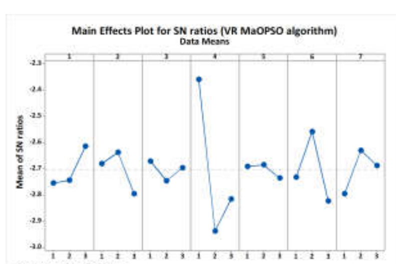

(e) VR MaOPSO algorithm

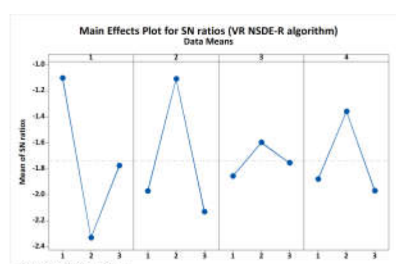

(f) VR NSDE-R algorithm

Figure 4: The main effects plots for signal-to-noise ratio of many-objective metaheuristic algorihtms

Table 2: The optimal parameter levels of the many-objective algorithms

Algorithm	Parameter number	Parameter name	Optimal level	Algorithm	Parameter number	Parameter name	Optimal level
NSGA-III	1	N_{pop}	20	VR NSGA-III	1	N_{pop}	30
	2	$\|H\|$	30		2	$\|H\|$	30
	3	P_{cr}	0.70		3	P_{cr}	0.95
	4	P_{mu}	0.10		4	P_{mu}	0.50
MaOPSO	1	N_{pop}	25	VR MaOPSO	1	N_{pop}	30
	2	$Arch_{size}$	40		2	$Arch_{size}$	35
	3	$\|H\|$	45		3	$\|H\|$	30
	4	C_1	2		4	C_1	1
	5	C_2	1.5		5	C_2	2
	6	w	0.90		6	w	0.95
	7	$wdamp$	0.95		7	$wdamp$	0.99
NSDE-R	1	N_{pop}	25	VR NSDE-R	1	N_{pop}	20
	2	P_{cr}	0.99		2	P_{cr}	0.95
	3	$\|H\|$	45		3	$\|H\|$	45
	4	F	1.40		4	F	0.90

5.4. Results discussion

The input parameters of algorithms are set to the obtained optimal values by the Taguchi method. As the results may vary across different executions, each algorithm is run five times for each case to obtain reliable and statistically significant results. For the VR algorithms, the best clinically acceptable solution is the considered desired point. According to the high importance of clinically acceptable solutions in the multiobjective DAAO problem, we separate these solutions from the other Pareto solutions for each algorithm and only consider them in our comparisons.

First, the overall non-dominated vector generation measure is presented in Table 3. As can be seen in the table, the overall non-dominated vector generation measure of each VR algorithm is better than the classical versions. This means that the VR algorithms consider the DVH criteria in their search process using the input desired point. The change in the search direction of algorithms can also be seen in the parallel coordinate plots of algorithms, which are shown in Figure 5.

The normalized parallel coordinated plot is a data visualization tool that is commonly used to represent the results of many-objective algorithms. The plot consists of multiple parallel axes, each representing an objective function, and a line connecting the values of each objective function for each Pareto solution. The data is normalized by dividing each objective by the range of values for that objective. This results in a plot displaying objectives on the same scale. As can be seen in Figure 5, the number of Pareto solutions with lower values of the PTV objective function are increased in the VR algorithms compared to their classical versions.

Table 3: The overall non-dominated vector generation measure results of the many-objective algorithms

Case	NSGA-III	VR NSGA-III	MaOPSO	VR MaOPSO	NSDE-R	VR NSDE-R
#1	7.40	12.20	6.40	**12.60**	2.75	3.20
#2	4.60	**6.80**	**6.80**	6.60	1.40	2.00
#3	3.60	7.00	4.00	**9.00**	2.00	2.00
#4	**7.00**	3.80	4.00	5.00	2.25	3.80
#5	3.80	8.80	8.00	**8.40**	1.50	3.00
#6	4.40	9.80	7.00	**11.20**	2.67	4.60
#7	2.40	4.20	2.20	**6.00**	2.00	1.75
#8	4.60	11.00	8.40	**12.60**	2.60	3.20
#9	3.40	6.80	2.60	**7.00**	1.67	1.50
#10	4.60	5.80	6.40	**8.60**	1.80	4.00
Average	4.58	7.62	5.58	**8.70**	2.06	2.90

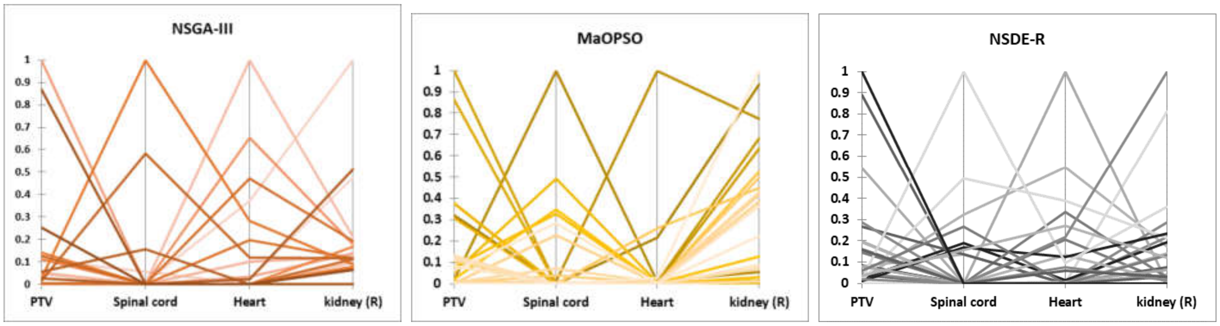

(a) NSGA-III algorithm (b) MaOPSO algorithm (c) NSDE-R algorithm

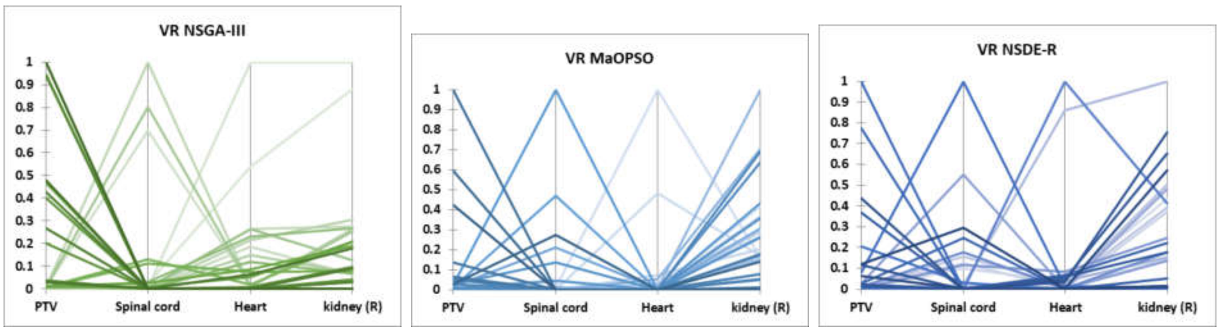

(d) VR NSGA-III algorithm (e) VR MaOPSO algorithm (f) VR NSDE-R algorithm

Figure 5: Parallel coordinate plot of many-objective algorithms for Case #2

Next, the algorithms are compared using the diversity measure. The diversity of clinically acceptable solutions of algorithms is presented in Table 4. As expected, the increase in overall non-dominated vector generation of VRPP algorithms causes an increase in the diversity measure. Such increases in diversity provide more options for clinical decision-makers to select the proper treatment plan. Similar to overall non-dominated vector generation, the maximum diversity belongs to the VR MaOPSO algorithm.

Spacing is the third measure for the performance comparison of algorithms, and the results are provided in Table 5. The results show that the spacing measure of classical algorithms is better than their new versions. As noted by Audet et al. (2021), when the Pareto solutions form separate clusters, the spacing measure becomes less effective. In other words, the spacing measure is highly

Table 4: The diversity measure results of the many-objective algorithms

Case	NSGA-III	VR NSGA-III	MaOPSO	VR MaOPSO	NSDE-R	VR NSDE-R
#1	15.26	**25.73**	10.33	21.20	6.88	8.22
#2	7.52	11.06	13.55	**14.83**	4.32	5.64
#3	7.80	9.58	8.97	**17.48**	2.65	4.32
#4	7.03	7.88	9.55	**9.88**	2.44	9.64
#5	3.81	11.55	10.74	**12.63**	3.92	4.53
#6	9.55	13.56	17.37	**22.50**	8.44	9.13
#7	7.11	9.30	3.75	**13.71**	4.93	5.63
#8	9.86	18.02	15.86	**23.21**	8.60	10.18
#9	7.88	14.36	7.70	**17.60**	4.94	7.22
#10	9.43	10.28	14.75	**14.99**	4.28	10.41
Average	8.53	14.03	11.26	**16.80**	5.14	7.49

sensitive to the distribution of mutual distances between solutions on the Pareto front. Thus, while an algorithm may yield a higher number of solutions and greater diversity, it can still have a higher spacing measure due to the particular distribution of the solutions on the front. For the presented algorithm, an increase in the number of clinically acceptable solutions results in more variation in the mutual distances between the solutions, leading to an increase in the value of the spacing measure for VR algorithms. MaOPSO discovers more clinically acceptable solutions with greater diversity, resulting in an increase in the spacing measure for this algorithm. The NSDE-R algorithm achieves the minimum spacing.

Table 5: The spacing measure results of the many-objective algorithms

Case	NSGA-III	VR NSGA-III	MaOPSO	VR MaOPSO	NSDE-R	VR NSDE-R
#1	0.79	0.96	**0.38**	0.74	0.55	0.55
#2	0.78	0.91	0.92	0.81	**0.12**	0.35
#3	1.15	0.61	0.30	0.61	**0.00**	0.79
#4	0.53	0.64	0.70	**0.52**	0.61	1.01
#5	0.45	1.10	0.81	0.88	**0.00**	0.36
#6	0.92	0.88	**0.61**	0.98	0.63	0.74
#7	0.29	0.75	0.35	0.58	**0.14**	0.35
#8	0.70	0.95	0.49	0.82	**0.39**	0.62
#9	0.58	0.76	0.22	0.87	**0.00**	0.35
#10	0.79	0.61	0.68	0.52	**0.03**	0.35
Average	0.70	0.82	0.55	0.73	**0.25**	0.55

As the last measure for the comparison of algorithms, the CPU times are summarized in Table 6. The CPU time of classical many-objective algorithms is lower than that of the VR algorithms. Although the VR algorithms require more CPU time, the increase is not significant. The results show that the difference between NSGA-III, MaOPSO, and NSDE-R with their VR versions is approximately 5.24%, 5.02%, and 5.34%, respectively. Such increases in CPU time do not significantly affect the performance, and the VR algorithms can search for solutions in a reasonable time. Moreover, the MaOPSO algorithm, which also obtains higher-quality solutions, has the maximum average CPU time.

The boxplots of considered measures are presented in Figure 6 to provide a better insight into the performance of many-objective algorithms. Moreover, to provide a better insight, the CT scan

Table 6: The CPU time measure results of the many-objective algorithms (S)

Case	NSGA-III	VR NSGA-II	MaOPSO	VR MaOPSO	NSDE-R	VR NSDE-R
#1	**121.17**	126.80	163.11	173.55	132.75	139.13
#2	**76.31**	81.08	124.95	131.37	91.47	96.14
#3	190.90	201.74	213.55	227.10	**177.26**	186.86
#4	141.15	149.98	162.11	172.02	**131.26**	138.25
#5	135.95	141.53	157.96	167.51	**120.06**	126.06
#6	**114.64**	119.36	152.72	158.91	117.87	122.25
#7	173.66	182.45	202.20	208.27	**156.48**	166.12
#8	182.77	193.32	214.43	224.88	**167.90**	179.42
#9	183.82	193.05	219.63	230.83	**172.05**	183.18
#10	150.95	159.32	192.03	198.74	**144.53**	150.43
Average	147.13	154.86	180.27	189.32	**141.16**	148.78

for one of the obtained clinically acceptable solutions of each algorithm for Case #2 is shown in Figure 7.

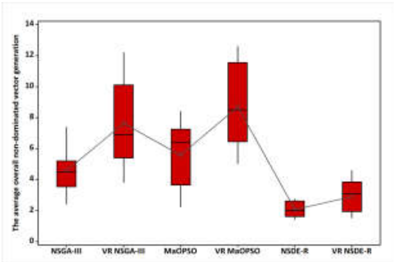

(a) Overall non-dominated vector generation measure

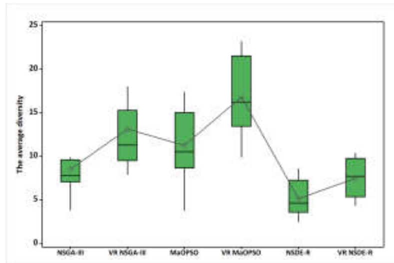

(b) Diversity measure

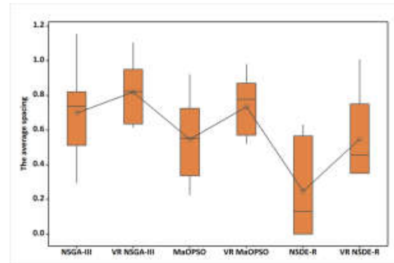

(c) Spacing measure

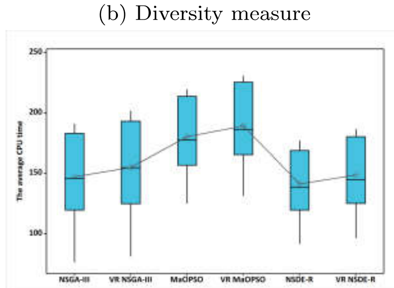

(d) CPU time measure

Figure 6: The boxplot considered measures for comparison of many-objective algorithms

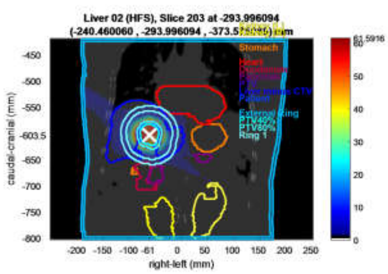

(a) NSGA-III algorithm

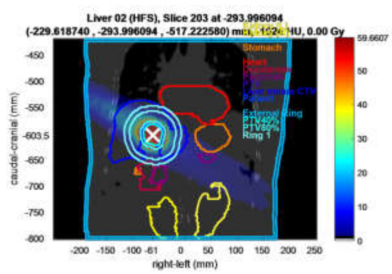

(b) VR NSGA-III algorithm

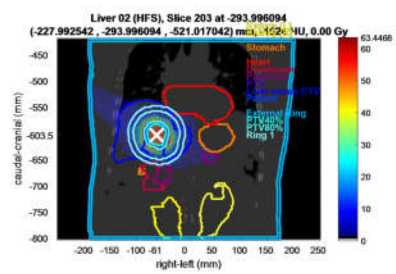

(c) MaOPSO algorithm

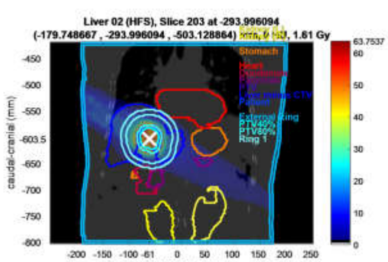

(d) VR MaOPSO algorithm

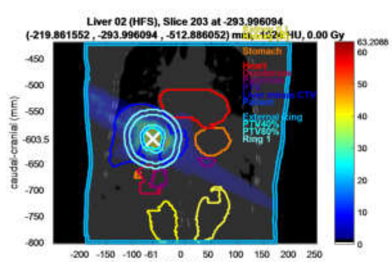

(e) NSDE-R algorithm

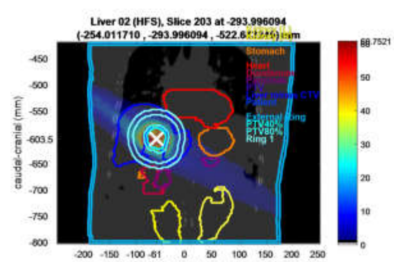

(f) VR NSDE-R algorithm

Figure 7: The CT scan of an obtained clinically acceptable solution for Case #2

5.5. *Comparison to NSGA-II in the literature*

Finally, we have compared our most powerful many-objective algorithm, VR MaOPSO, to one of the state-of-the-art multiobjective algorithms in the literature, NSGA-II, to identify clinically acceptable solutions. NSGA-II has been designed and implemented for several IMRT treatment planning problems in recent years, including BOO, FMO, and DAO (Cao et al., 2011; Schreibmann et al., 2004; Li et al., 2009). To this end, we implement the NSGA-II algorithm for all 10 liver cases of the TROTS data set. Table 7 presents VR MaOPSO and NSGA-II comparison results in terms of the considered performance measures.

Table 7: The comparison of VR MaOPSO and NSGA-II algorithms

Case	Overall non-dominated vector generation		Diversity		Spacing		CPU time	
	VR MaOPSO	NSGA-II	VR MaOPSO	NSGA-II	VR MaOPSO	NSGA-II	VR MaOPSO	NSGA-II
#1	**12.6**	3.1	**21.20**	6.60	0.74	**0.61**	**173.55**	208.06
#2	**6.6**	2.2	**14.83**	3.31	0.81	**0.50**	**131.37**	136.23
#3	**9.0**	1.8	**17.48**	3.16	**0.61**	0.90	**227.10**	338.43
#4	**5.0**	2.8	**9.88**	2.81	0.52	**0.36**	**172.02**	246.18
#5	**8.4**	1.5	**12.63**	1.81	0.88	**0.24**	**167.51**	239.16
#6	**11.2**	2.0	**22.50**	4.06	0.98	**0.53**	**158.91**	210.59
#7	**6.0**	1.0	**13.71**	3.12	0.58	**0.16**	**208.27**	296.22
#8	**12.6**	2.1	**23.21**	4.70	0.82	**0.47**	**224.88**	322.08
#9	**7.0**	1.6	**17.60**	3.50	0.87	**0.36**	**230.83**	335.93
#10	**8.6**	2.3	**14.99**	4.20	**0.52**	0.62	**198.74**	260.40
Average	**8.7**	3.1	**16.80**	3.73	0.73	**0.47**	**189.31**	259.33

The results indicate that VR-MaOPSO outperforms NSGA-II in terms of its ability to produce clinically acceptable solutions within a shorter time frame. We observed that the VR-MaOPSO algorithm generates a larger number of diverse solutions than the NSGA-II algorithm. Additionally, consistent with prior comparisons, the NSGA-II algorithm demonstrates a lower spacing measure due to its limited number of acceptable solutions. Overall, these findings emphasize the efficacy of the VR-MaOPSO algorithm in addressing multi-objective optimization problems that have clinical applications.

6. Conclusion

This paper proposed a multiobjective framework for the DAAO problem in IMRT treatment planning, which simultaneously optimizes the beam directions, intensity map, and MLC sequences. The proposed framework enables the clinical decision-makers to consider each desired organ of a patient as an objective function and helps them to determine the proper plan from a set of Pareto solutions. The problem is formulated using a non-linear programming mathematical model. Regarding the nonlinearity, dimension, and the possible number of objective functions, an application of reference point-based many-objective metaheuristic algorithms is presented as the solution approach. First, three classical many-objective metaheuristic algorithms are designed and implemented, including NSGA-III, MaOPSO, and NSDE-R. Next, the importance of clinical criteria motivated us to modify these classical algorithms and present a new version based on the decision-makers preferences. For this goal, the new extensions of algorithms were presented as the VR of many-objective algorithms. These algorithms can modify the algorithms by changing the position of reference points to actively consider the decision-maker preferences during the search procedure.

The performance of six proposed many-objective algorithms in solving the multiobjective DAAO problem was investigated using 10 liver cases data from the TROTS dataset. We calibrated the input parameters of many-objective metaheuristics utilizing the Taguchi design of experiments as a systematic statistical method. Four performance measures including overall non-dominated vector generation measure, diversity, spacing, and CPU time were used to compare the algorithms. The analysis of the results revealed that the new extended algorithms could successfully consider the decision-makers preferences in a proper manner. More specifically, the algorithms can improve the number and diversity of clinically acceptable solutions while the increase in computational cost is negligible. It is noteworthy to mention that the quality of the obtained solutions by VR MaOPSO is higher than the other algorithms in terms of clinical criteria.

For the extension of the current paper, several directions can be considered. The present multiobjective DAAO problem assumes that all parameters are in deterministic form. Reformulating the model under uncertainty in some parameters, such as the tumor progress status or breathing motion, is interesting. In addition, we use a single type of objective function for all organs. Different varieties of objective functions, such as biological ones can be considered for organs in the multiobjective DAAO problem. From the solution methodology viewpoint, machine learning algorithms, such as Q-learning, can be utilized to adapt reference points in VR algorithms.

References

Atun, R., Jaffray, D. A., Barton, M. B., Bray, F., Baumann, M., Vikram, B., Hanna, T. P., Knaul, F. M., Lievens, Y., Lui, T. Y., et al. (2015). Expanding global access to radiotherapy. *The lancet oncology*, 16(10):1153–1186.

Audet, C., Bigeon, J., Cartier, D., Le Digabel, S., and Salomon, L. (2021). Performance indicators in multiobjective optimization. *European Journal of Operational Research*, 292(2):397–422.

Bader, J. and Zitzler, E. (2010). A hypervolume-based optimizer for high-dimensional objective spaces. In *New developments in multiple objective and goal programming*, pages 35–54. Springer.

Bahr, G., Kereiakes, J. G., Horwitz, H., Finney, R., Galvin, J., and Goode, K. (1968). The method of linear programming applied to radiation treatment planning. *Radiology*, 91(4):686–693.

Bertsimas, D., Cacchiani, V., Craft, D., and Nohadani, O. (2013). A hybrid approach to beam angle optimization in intensity-modulated radiation therapy. *Computers & Operations Research*, 40(9):2187–2197.

Breedveld, S., Craft, D., Van Haveren, R., and Heijmen, B. (2019). Multi-criteria optimization and decision-making in radiotherapy. *European Journal of Operational Research*, 277(1):1–19.

Breedveld, S. and Heijmen, B. (2017). Data for TROTS–the radiotherapy optimisation test set. *Data in brief*, 12:143–149.

Breedveld, S., Storchi, P. R., and Heijmen, B. J. (2009). The equivalence of multi-criteria methods for radiotherapy plan optimization. *Physics in Medicine & Biology*, 54(23):7199.

Breedveld, S., Storchi, P. R., Voet, P. W., and Heijmen, B. J. (2012). iCycle: Integrated, multicriterial beam angle, and profile optimization for generation of coplanar and noncoplanar IMRT plans. *Medical Physics*, 39(2):951–963.

Cabrera, G., Ehrgott, M., Mason, A., and Philpott, A. (2014). Multi-objective optimisation of positively homogeneous functions and an application in radiation therapy. *Operations Research Letters*, 42(4):268–272.

Cabrera-Guerrero, G., Ehrgott, M., Mason, A. J., and Raith, A. (2018). A matheuristic approach to solve the multiobjective beam angle optimization problem in intensity-modulated radiation therapy. *International Transactions in Operational Research*, 25(1):243–268.

Cabrera-Guerrero, G. and Lagos, C. (2022). Comparing multi-objective local search algorithms for the beam angle selection problem. *Mathematics*, 10(1):159.

Cáceres, L. P., Araya, I., and Cabrera-Guerrero, G. (2021). Stochastic local search for the direct aperture optimisation problem. *Expert Systems with Applications*, 182:115206.

Cao, R., Pei, X., Wang, J., and Wu, Y. (2011). Su-e-t-869: Direct aperture optimization based on multi-objective evolutionary algorithm in intensity modulated radiation therapy. *Medical Physics*, 38(6Part24):3691–3691.

Chan, T. C. and Mišić, V. V. (2013). Adaptive and robust radiation therapy optimization for lung cancer. *European Journal of Operational Research*, 231(3):745–756.

Craft, D. (2013). Multi-criteria optimization methods in radiation therapy planning: a review of technologies and directions. *arXiv preprint arXiv:1305.1546*.

Craft, D., Halabi, T., Shih, H. A., and Bortfeld, T. (2007). An approach for practical multiobjective IMRT treatment planning. *International Journal of Radiation Oncology Biology Physics*, 69(5):1600–1607.

Das, I. and Dennis, J. E. (1998). Normal-boundary intersection: A new method for generating the pareto surface in nonlinear multicriteria optimization problems. *SIAM journal on optimization*, 8(3):631–657.

Deb, K. and Jain, H. (2013). An evolutionary many-objective optimization algorithm using reference-point-based nondominated sorting approach, part I: solving problems with box constraints. *IEEE transactions on evolutionary computation*, 18(4):577–601.

Deb, K., Pratap, A., Agarwal, S., and Meyarivan, T. (2002). A fast and elitist multiobjective genetic algorithm: NSGA-II. *IEEE Transactions on Evolutionary Computation*, 6(2):182–197.

Dursun, P., Taşkın, Z. C., and Altınel, İ. K. (2019). Using branch-and-price to determine optimal treatment plans for volumetric modulated arc therapy (VMAT). *Computers & Operations Research*, 110:1–17.

Ehrgott, M., Güler, Ç., Hamacher, H. W., and Shao, L. (2010). Mathematical optimization in intensity modulated radiation therapy. *Annals of Operations Research*, 175(1):309–365.

Fallahi, A., Mahnam, M., and Niaki, S. T. A. (2022a). Direct aperture optimization for intensity modulated radiation therapy: Two calibrated metaheuristics and liver cancer case study. *International Journal of Industrial Engineering & Production Research*, 33(2):1–14.

Fallahi, A., Mahnam, M., and Niaki, S. T. A. (2022b). A discrete differential evolution with local search particle swarm optimization to direct angle and aperture optimization in IMRT treatment planning problem. *Applied Soft Computing*, page 109798.

Fang, Y., Liu, Q., Li, M., Laili, Y., and Pham, D. T. (2019). Evolutionary many-objective optimization for mixed-model disassembly line balancing with multi-robotic workstations. *European Journal of Operational Research*, 276(1):160–174.

Fiege, J., McCurdy, B., Potrebko, P., Champion, H., and Cull, A. (2011). PARETO: a novel evolutionary optimization approach to multiobjective IMRT planning. *Medical Physics*, 38(9):5217–5229.

Figueiredo, E. M., Ludermir, T. B., and Bastos-Filho, C. J. (2016). Many objective particle swarm optimization. *Information Sciences*, 374:115–134.

Freitas, J. C. d., de Oliveira Florentino, H., dos Santos Benedito, A., and Cantane, D. R. (2020). Optimization model applied to radiotherapy planning problem with dose intensity and beam choice. *Applied Mathematics and Computation*, 387:124786.

Habib, R. R., Yeung, J., Darko, J., Osei, E., and Mahmoudzadeh, H. (2022). Optimization of sliding windows IMRT treatment planning. *IISE Transactions on Healthcare Systems Engineering*, 12(3):180–192.

Hou, Q., Wang, J., Chen, Y., and Galvin, J. M. (2003). Beam orientation optimization for IMRT by a hybrid method of the genetic algorithm and the simulated dynamics. *Medical Physics*, 30(9):2360–2367.

Jaszkiewicz, A. (2018). Many-objective pareto local search. *European Journal of Operational Research*, 271(3):1001–1013.

Jee, K.-W., McShan, D. L., and Fraass, B. A. (2007). Lexicographic ordering: intuitive multicriteria optimization for IMRT. *Physics in Medicine & Biology*, 52(7):1845.

Kalantzis, G. and Lei, Y. (2014). A self-tuned bat algorithm for optimization in radiation therapy treatment planning. In *15th IEEE/ACIS International Conference on Software Engineering, Artificial Intelligence, Networking and Parallel/Distributed Computing (SNPD)*, pages 1–6. IEEE.

Kalantzis, G., Shang, C., Lei, Y., and Leventouri, T. (2016). Investigations of a GPU-based levy-firefly algorithm for constrained optimization of radiation therapy treatment planning. *Swarm and Evolutionary Computation*, 26:191–201.

Küfer, K.-H., Hamacher, H. W., and Bortfeld, T. (2000). A multicriteria optimization approach for inverse radiotherapy planning. In *The Use of Computers in Radiation Therapy*, pages 26–28. Springer.

Li, G., Lin, L., and Li, Z. (2009). An improved NSGA-II algorithm for the optimization of IMRT inverse planning. In *2009 2nd International Conference on Biomedical Engineering and Informatics*, pages 1–3. IEEE.

Li, Y., Yao, D., Chen, W., Zheng, J., and Yao, J. (2005a). Ant colony system for the beam angle optimization problem in radiotherapy planning: a preliminary study. In *2005 IEEE Congress on Evolutionary Computation*, volume 2, pages 1532–1538. IEEE.

Li, Y., Yao, D., Yao, J., and Chen, W. (2005b). A particle swarm optimization algorithm for beam angle selection in intensity-modulated radiotherapy planning. *Physics in Medicine & Biology*, 50(15):3491.

Li, Y., Yao, D., Zheng, J., and Yao, J. (2005c). A modified genetic algorithm for the beam angle optimization problem in intensity-modulated radiotherapy planning. In *International Conference on Artificial Evolution (Evolution Artificielle)*, pages 97–106. Springer.

Li, Y., Yao, J., and Yao, D. (2003). Genetic algorithm based deliverable segments optimization for static intensity-modulated radiotherapy. *Physics in Medicine & Biology*, 48(20):3353.

Lim, G. J., Kardar, L., Ebrahimi, S., and Cao, W. (2020). A risk-based modeling approach for radiation therapy treatment planning under tumor shrinkage uncertainty. *European Journal of Operational Research*, 280(1):266–278.

Lin, K.-M., Ehrgott, M., and Raith, A. (2017). Integrating column generation in a method to compute a discrete representation of the non-dominated set of multi-objective linear programmes. *4OR*, 15(4):331–357.

Mahnam, M., Gendreau, M., Lahrichi, N., and Rousseau, L.-M. (2017). Simultaneous delivery time and aperture shape optimization for the volumetric-modulated arc therapy (VMAT) treatment planning problem. *Physics in Medicine & Biology*, 62(14):5589.

Mahnam, M., Gendreau, M., Lahrichi, N., and Rousseau, L.-M. (2019). Integrating DVH criteria into a column generation algorithm for VMAT treatment planning. *Physics in Medicine & Biology*, 64(8):085008.

Mueller, S., Guyer, G., Risse, T., Tessarini, S., Aebersold, D. M., Stampanoni, M. F., Fix, M. K., and Manser, P. (2022). A hybrid column generation and simulated annealing algorithm for direct aperture optimization. *Physics in Medicine & Biology*, 67(7):075003.

Nazareth, D. P. and Spaans, J. D. (2015). First application of quantum annealing to IMRT beamlet intensity optimization. *Physics in Medicine & Biology*, 60(10):4137.

Reddy, S. R. and Dulikravich, G. S. (2019). Many-objective differential evolution optimization based on reference points: NSDE-R. *Structural and Multidisciplinary Optimization*, 60(4):1455–1473.

Ripsman, D. A., Purdie, T. G., Chan, T. C., and Mahmoudzadeh, H. (2022). Robust direct aperture optimization for radiation therapy treatment planning. *INFORMS Journal on Computing*, 34(4):2017–2038.

Rocha, H., Dias, J. M., Ferreira, B. C., and Lopes, M. (2012). Discretization of optimal beamlet intensities in IMRT: a binary integer programming approach. *Mathematical and Computer Modelling*, 55(7-8):1969–1980.

Romeijn, H. E., Ahuja, R. K., Dempsey, J. F., and Kumar, A. (2005). A column generation approach to radiation therapy treatment planning using aperture modulation. *SIAM Journal on Optimization*, 15(3):838–862.

Sadeghi, J., Sadeghi, S., and Niaki, S. T. A. (2014). A hybrid vendor managed inventory and redundancy allocation optimization problem in supply chain management: An NSGA-II with tuned parameters. *Computers & Operations Research*, 41:53–64.

Sahinkoc, H. M. and Bilge, Ü. (2022). A reference set based many-objective co-evolutionary algorithm with an application to the knapsack problem. *European Journal of Operational Research*, 300(2):405–417.

Salari, E. and Unkelbach, J. (2013). A column-generation-based method for multi-criteria direct aperture optimization. *Physics in Medicine & Biology*, 58(3):621.

Schreibmann, E., Lahanas, M., Xing, L., and Baltas, D. (2004). Multiobjective evolutionary optimization of the number of beams, their orientations and weights for intensity-modulated radiation therapy. *Physics in Medicine & Biology*, 49(5):747.

Shahidi-Zadeh, B., Tavakkoli-Moghaddam, R., Taheri-Moghadam, A., and Rastgar, I. (2017). Solving a bi-objective unrelated parallel batch processing machines scheduling problem: A comparison study. *Computers & Operations Research*, 88:71–90.

Shao, L. and Ehrgott, M. (2008). Approximately solving multiobjective linear programmes in objective space and an application in radiotherapy treatment planning. *Mathematical Methods of Operations Research*, 68(2):257–276.

Shepard, D. M., Ferris, M. C., Olivera, G. H., and Mackie, T. R. (1999). Optimizing the delivery of radiation therapy to cancer patients. *Siam Review*, 41(4):721–744.

Sun, J., Zhang, G., Lu, J., and Zhang, W. (2021). A hybrid many-objective evolutionary algorithm for flexible job-shop scheduling problem with transportation and setup times. *Computers & Operations Research*, 132:105263.

Taşkın, Z. C. and Cevik, M. (2013). Combinatorial benders cuts for decomposing IMRT fluence maps using rectangular apertures. *Computers & Operations Research*, 40(9):2178–2186.

Vesikar, Y., Deb, K., and Blank, J. (2018). Reference point based NSGA-III for preferred solutions. In *2018 IEEE symposium series on computational intelligence (SSCI)*, pages 1587–1594. IEEE.

Webb, S. (1994). Optimizing the planning of intensity-modulated radiotherapy. *Physics in Medicine & Biology*, 39(12):2229.

Wilkens, J. J., Alaly, J. R., Zakarian, K., Thorstad, W. L., and Deasy, J. O. (2007). IMRT treatment planning based on prioritizing prescription goals. *Physics in Medicine & Biology*, 52(6):1675.

Zaghian, M., Lim, G. J., and Khabazian, A. (2018). A chance-constrained programming framework to handle uncertainties in radiation therapy treatment planning. *European Journal of Operational Research*, 266(2):736–745.

Zitzler, E. and Künzli, S. (2004). Indicator-based selection in multiobjective search. In *International conference on parallel problem solving from nature*, pages 832–842. Springer.